Porous CS based membranes with improved antimicrobial properties for the treatment of infected wound in veterinary applications

Materials Science and Engineering C,

volume 60, 2016, DOI 10.1016/j.msec.2015.11.065

0928-4931

Porous CS based membranes with improved antimicrobial properties for the treatment of infected wound in veterinary applications.

C. Tonda-Turo[a]*, F.Ruini[a], M. Argentati[a,b], N. Di Girolamo[b], P. Robino[c], P. Nebbia[c], G.Ciardelli[a]

[a] Department of Mechanical and Aerospace Engineering, Politecnico di Torino, Corso Duca degli Abruzzi 24, 10129 Turin, Italy

[b] Clinic for Exotic Animals, CVS, Via Sandro Giovannini 53, 00137 Rome, Italy

[c] Department of Veterinary Sciences, University of Turin, Largo Braccini 2, 10095 Grugliasco (Turin), Italy

[*] Dr. Chiara Tonda-Turo

Department of Mechanical and Aerospace Engineering

Politecnico di Torino

Corso Duca degli Abruzzi 24, Turin, Italy

telephone number: 0039 0903395

fax number: 0039 0906999

e-mail address: *chiara.tondaturo@polito.it*

Abstract

Recently, much attention has been given to the use of innovative solution for the treatment of infected wounds in animals. Current applied treatments are often un-effective leading to infection propagation and animal death. Novel engineered membranes based on chitosan (CS) can be prepared to combine local antimicrobial effect, high flexibility and easy manipulation.

In this work, CS crosslinked porous membranes with improved antimicrobial properties were prepared via freeze-drying technique to promote wound healing and to reduce the bacterial proliferation in infected injuries. Silver nanoparticles (AgNPs) and gentamicin sulphate (GS) were incorporated into the CS matrices to impart antibacterial properties on a wild range of strains. CS based porous membranes were tested for their physicochemical, thermal, mechanical as well as swelling and degradation behavior at physiological condition. Additionally, GS release profile was investigated, showing a moderate burst effect in the first days followed by a decreasing release rate which was maintained for at least 56 days. Moreover, porous membranes loaded with GS or AgNPs showed good bactericidal activity against both of

gram-positive and gram-negative bacteria. The bacterial strains used in this work were collected in chelonians after carapace injuries to better mimic the environment after trauma.

Keywords: antibacterial agent, chitosan, gentamicin, silver nanoparticles, wound healing

1. Introduction

Infected injures are very common in animals and the recurring bacterial proliferation on the wound site may lead to animal's death for a variety of reasons, including internal hemorrhage, organ damage and sepsis. One common occurrence of infection-related animal death is the shell trauma of chelonians.

Shell trauma is one of the most common pathological conditions encountered in chelonians and it occurs with different seriousness degrees [1]. Carapace injuries arise mostly from dog bites, automobile and mower accidents, but can also result from falls [1]. Shell trauma may result in shell fractures with or without loss of bone tissue. In case of shell fracture without loss of bone tissue, closure of the fracture is usually enough to permit resolution of the wound while in case of severe fracture with loss of bone tissue, it is necessary to replace –at least temporarily- the tissue loss, as it will not regenerate spontaneously [2]. To treat chelonian carapace injuries, two clinical approaches are currently employed: i) the immediate closure of the shell by means of screws, plates and bone cements or epoxy resins [1, 3-7] or ii) the periodical direct medication of the wound through wet-to-dry bandages [1, 8], vacuum assisted closure (VAC) [9, 10], platelet-rich-plasma (PRP) treatment [11, 12] or ointments [13, 14]. In the former, the external fixation by means of screws and bone plates is used when wound contamination and infection have been prevented and there is no loss of bone tissue [15, 16] while cements/ epoxy resins are applied to fill bone missing zone [6, 7, 14, 17]. However, epoxy resins may cause an excessive tissue heating due to the exothermic nature of the resin polymerization process, they may require potentially toxic solvents for their removal [18] and they may increase the risk of contaminations that results in infection and sepsis [19]. In the latter treatment, turtle wound is left open in order to periodically disinfect and medicate it. Wet-to-dry bandages are generally used: the primary layer of gauzes is moist with sterile saline or dilute antiseptic solution and is allowed to dry out before its removal; however, dry gauzes are preferred in the presence of wound exudates and lets out necrotic tissue or debris [20]. However, there are many drawbacks associated with bandages, such as the damage of healthy tissue, the presence of disperse bacteria and fibers in the wound bed after the removal of gauzes [10]. The use of VAC technology consists on the application of an open-cell foam over the wound, secured to the site with adhesive occlusive drape, to which a suction system is attached [9]. With a constant negative pressure of about 125 mmHg [1] fluids can be collected from the wound permitting the exudate and bacteria removal and

granulation tissue formation [21]. Disadvantages include the initial price and the need of proper training to use the equipment. Moreover, VAC technology is unsuitable in the case of a gross infection, lack of wound haemostasis, unprotected vascular anastomoses, foam placement over vessels, the presence of necrotic tissue with scar, exposed organs and malignancy in the wound bed [22]. PRP is a platelet concentrate derived from blood centrifugation procedures [11] which locally delivers high amounts of growth factors involved in haemostasis and cell proliferation (fibroblasts, osteoblasts, endothelial cells), promoting the wound healing process [23]. PRP gel must be applied onto the wound surface and is to be protected by a sterile gauze for 48 hours [12], working as a barrier against external microorganisms. Disadvantages of this technique include the need of an initial investment, the need of a proper training to use the equipment and the lack of a thorough understanding of the biologic interactions among PRP gel and the animal tissue. Among ointments, honey and sugar, petroleum impregnated gauzes, triple antibiotic ointment, GS cream and a variety of silver based products have been widely used in managing chelonian shell wound to prevent infection, maintain moisture, enhance healing, or facilitate debridement [14, 24]. Silver (Ag) is known for its broad antibacterial spectrum; it can be used as ointment and cream (silver sulfadiazine) [8], or it can be loaded in matrices as nanoparticles for its controlled release [25, 26]. Unfortunately, even if it shows an high antimicrobial activity, Ag has a potential toxic effect at higher dosage [27]. On the contrary, honey and sugar are cheaper and effective against a wide variety of Gram-positive and Gram-negative bacteria, explicating their action by hydrogen peroxide release [28, 29]. GS also exherts antibacterial effects against both Gram-positive and Gram-negative bacteria [30] but it has a potential nephrotoxic effect depending on its concentrations [31].

In this contest, skin tissue engineering (TE) could be a promising alternative approach to treat chelonian shell injuries and recently few studies have been reported [14, 32]. The final aim of the TE scaffold is to protect the injury during the regeneration process and to improve dermal and epidermal tissue regeneration [33]. The implantation of biodegradable membranes is encourage since they completely cover the wound site, avoiding dirt and bacterial infiltration, and their removal is not required at the end of the treatment due to the material biodegradability [33]. Moreover, biodegradable membranes can act as drug delivery systems loading antibiotic agents that are locally released during membranes degradation [34]. The localized drug release achieved using biodegradable membranes guarantees lower antibiotic concentrations compared to systemic therapy due to the direct drug release in the wound site, thus assuming a lower toxicity. Alginates, hydrocolloids, hydrogels and foams are the most popular wound dressing in veterinary applications [20]. Among the natural polymers, CS (alone or coupled with antimicrobial or antibiotic agents) has been widely used in wound management both in humans and animals [35, 36].

In this study, CS based porous membranes with improved antimicrobial properties were developed to promote the wound healing process and to reduce the bacterial proliferation in chelonian shell injury site. To improve the

mechanical properties and water stability of CS, dibasic sodium phosphate (DSP) and (3-Glycidoxypropyl)methyldiethoxysilane (GPTMS) were used as crosslinking agents. Furthermore, GS and AgNPs were loaded into the developed membranes to improve the antibacterial effect against Gram-positive and Gram-negative bacteria and to guarantee drug controlled release in time and in space without exceeded the toxic dosage for systemic circulation. The obtained porous membranes were analyzed for their physicochemical and morphological properties by scanning electron microscopy (SEM), Energy Dispersive X-ray Spectrometry (EDS) and thermogravimetric analysis (TGA) while their mechanical properties were evaluated by tensile and compressive tests. Swelling and dissolution degree were measured in media simulating physiological conditions. GS release from CS porous membranes was evaluated by means of UV-VIS spectroscopy, while the AgNPs release was indirectly investigated through *in vitro* antibacterial tests using five different bacteria lineages: *Staphylococcus aureus* (Gram-positive), *Escherichia coli* (Gram-negative) *Enterococcus faecalis* (Gram-positive), *Pseudomonas aeruginosa* (Gram-negative) and *Proteus mirabilis* (Gram-negative).

2. Experimental

2.1 Materials

CS (medium molecular weight, 75%-85% deacetylation degree), GPTMS, DSP, GS and AgNPs (<110 nm particle size) were supplied from Sigma Aldrich. All solvents used were of analytical grade and used without further purification.

2.2 Methods

CS was dissolved in acetic acid solution 0.5M to form a CS solution of 2.5% w/v. Four different typologies of CS based membranes were prepared according to the following procedures:

i. CS/GPTMS_DSP were obtained by adding GPTMS and DSP to the CS solution. GPTMS (50% w/w) was added to the CS solution and kept under magnetic stirring for about 1 hour. Afterward, DSP 1M solution (7.5 % v/v) was added dropwise to CS/GPTMS blend (one drop per second), maintained under stirring for about 10 minutes (CS/GPTMS_DSP).

ii. Membranes incorporating the antibiotic agent (CS/GPTMS_DSP_GS) were fabricated as follow. GS was dissolved in ultrapure water to obtain a solution with concentration of 3.5 mg/ml; then, the GS solution was poured dropwise onto the surface of CS/GPTMS_DSP porous membranes allowing its homogeneous absorption into the CS matrix. Finally, CS/GPTMS_DSP_GS samples were cooled down a second time at -20°C for 24 hours and then freeze-dried for 48 hours depending on the thickness of membranes.

iii. CS/GPTMS_DSP_AgNPs samples were obtained by adding AgNPs to CS/GPTMS_DSP solution. Three different amounts of AgNPs respect to the total amount of CS were added: 5%, 10% and 15% w/w (CS/GPTMS_DSP_AgNPs5, CS/GPTMS_DSP_AgNPs10 and CS/GPTMS_DSP_AgNPs15 respectively). Once AgNPs were incorporated, the solutions were kept under magnetic stirring till their homogeneity was reached. Then, CS/GPTMS_DSP and CS/GPTMS_DSP_AgNPs solutions were poured in different molds: 1) multiwell (2 ml in each well for compressive tests, 1 ml for the *in vitro* tests); 2) 10 cm-diameter Petri dishes (20 ml each) to obtain 2 mm thickness membranes for *in vivo* test; and 3) 12x12 cm-squared Petri dishes (90 ml) to obtain 5 mm thickness membranes for antibacterial tests. Once poured, samples were placed in a freezer at -20°C for 24 hours and then freeze-dried at -55°C for minimum 24 hours (48 hours for membranes with 5 mm thickness).

2.3 Sample characterization

2.3.1 Morphological characterization and element distribution

The external surface and fractured (in liquid nitrogen) sections morphology of CS/GPTMS_DSP, CS/GPTMS_DSP_AgNP5, CS/GPTMS_DSP_AgNP10, CS/GPTMS_DSP_AgNP15 and CS/GPTMS_DSP_GS porous membranes was observed by SEM (SEM LEO – 1430, Zeiss). Samples were sputter coated with gold in a undervacuum chamber prior to SEM-EDS examination.

Pore size was measured by analyzing the SEM images using an image software (ImageJ 1.43) and ten images for sample type were used. The ImageJ software measured the pore area; the pore size was calculated considering the pores as having circular shape with the same above measured area. Energy dispersive spectrometer (EDS) was applied to perform qualitative compositional analysis and the punctual elemental composition of materials with high spatial resolution was obtained.

2.3.2 Thermogravimetric analysis (TGA)

Thermal degradation was measured using a TA INSTRUMENT Q500 equipment to investigate the interaction between CS/GPTMS_DSP and the two antibacterial agents (AgNPs and GS) in terms of physic-chemical properties of the different samples. The experiments were performed with a 10-15 mg sample in aluminum pans under a dynamic nitrogen atmosphere between 40°C and 800 C. The experiments were run at a scanning rate of 10°C/min and obtained results were analyzed using TA Universal Analysis software.

2.3.3 Mechanical properties

Mechanical tests were performed to assess the mechanical behaviour of the membranes after implantation (flexibility, ability to cover the irregular shape of the trauma zone). Samples were tested in wet state since the *in vivo* implantation procedure on chelonians requires to soak the membranes with sterile 0.9% NaCl solution before application. In addition, the release of exudates from wound site in time maintains the developed scaffold in a moist environment. To have wet state, specimens were immersed in PBS (pH 7.4) for 10 minutes before testing. Both tensile and compressive tests were performed using MTS QTest/10 device equipped with load cells of 10 N and 50 N, respectively.

2.3.3.1 Tensile test

Rectangular strips of 10x30 mm size were cut from each typology of membranes. Then, samples were strained to break at a constant crosshead speed of 2 mm/min. Using the associated software Test Works, stress-strain curves were obtained, in which the elastic modulus was calculated from the slope of the first linear portion. To measure the thickness of the strips, digital calibrator was used and thicknesses were employed for determining the stress value. Four specimens for each kind of material were tested. The result was expressed as an average value ± standard deviation.

2.3.3.2 Compressive test

The compressive mechanical properties were performed on wet porous cylindrical scaffolds (1.2 cm diameter, 1cm height). All samples were compressed at a constant crosshead speed of 2 mm/min to approximately 80% of their original length. Four specimens for each kind of scaffold were tested. Young's modulus (E), collapse strength and strain (σ^* and ε^*, respectively) and collapse modulus (E^*) were measured from the stress-strain curves. E is the slope of the linear elastic regime, E^* is the slope of the collapse regime, σ^* and ε^* are respectively the stress and strain of transition from linear to collapse regime (determined from the intersection of E and E^* regression lines). The resulted values were expressed as an average value± standard deviation.

2.3.4 Water uptake and dissolution tests

The water uptake and dissolution behavior of porous samples were evaluated by immerging the samples in PBS (pH 7.4) at 37°C. The water uptake degree was measured after 1, 3, 6, 9 and 24 hours while the dissolution degree was evaluated after 1, 3, 5, 7, 14, 28 and 56 days. The water uptake percentage was calculated as:

$$\Delta W_s\,(\%) = (W_s - W_0)/W_0 * 100$$

where W_0 and W_S are the sample weights before and after swelling respectively. The dissolution percentage was calculated as:

$$\Delta W_d\,(\%) = (W_0 - W_d)/W_0 * 100$$

where W_d is the dried sample weight after dissolution. The solution pH was measured at the same time intervals during the swelling and the dissolution tests, and its stable value at around 7 (physiological pH) was verified. For each experimental time, three samples were measured and the results were expressed as averages value ± standard deviation.

2.3.5 GS release quantification

GS release from CS/GPTMS_DSP_GS membranes were carried out by UV-VIS spectroscopy (CARY 500 SCAN UV-VIS-NIR Spectrophotometer). Samples were immersed in 5 ml of PBS at pH 7.4 and GS concentration in the incubation media was measured after 1, 3, 6, 24 hours and 2, 7, 14, 28, 56 days. The GS release concentration was reported as a percentage respect to the initial concentration and it was calculated from the absorption values using the calibration curves that was prepared starting from GS solutions of known concentrations. UV spectra were recorded in a range of 400-200 nm. Five measures for sample were used and the data were reported as mean value ± standard deviation.

2.3.6 Antibacterial tests

The antibacterial properties of CS/GPTMS_DSP, CS/GPTMS_DSP_GS and CS/GPTMS_DSP_AgNP10 were tested against five pathogenic bacteria isolated from turtles wound infection: *Staphylococcus aureus*, *Escherichia coli*, *Enterococcus faecalis*, *Pseudomonas aeruginosa* and *Proteus mirabilis*. Samples (5 mm thickness) were prepared for antibacterial tests. Strains were stored in tryptone soy broth (TSB, Oxoid, Milano) with 20% glycerol at -80°C until needed. For experimental use, the stock cultures were grown on tryptone soy agar (TSA, Oxoid) slants, then each strain 2-3 colonies was transferred to 10 ml of TSB and incubated at 37°C for 18 hours to obtain early stationary phase cells. Cell cultures of each microorganism in stationary phase were diluted in TSB and incubated at 37°C until an optical density of $0.2x10^5$ colony-forming units (CFU/ml) at 600 nm was reached. Tubes with 10 ml of Mueller-Hinton broth (MHB, Oxoid) were inoculated with 100 µl of culture. Sample weighing 0.25 g were then cut into 1.5 cm^2 pieces and added to each tube. The tubes were then incubated at 37 °C for 18 hours. Depending on the turbidity of the tubes, serial dilutions with peptone water were made and plated in Petri dishes with 15 mL of TSA culture medium. Colonies (CFU) were counted after incubation at 37 °C for 18 hours. Three replicate plates were used per each dilution of broth.

2.3.7 Statistics

Results were expressed as an mean ± standard deviation. Statistical significance was calculated using analysis of variance (ANOVA). A comparison between two means was analyzed using Tukey's test with statistical significance level set at $p<0.05$.

Results and discussion

3.1 Morphological characterization and element distribution

In figure 1 the surfaces and the fractured sections of CS/GPTMS_DSP membranes loaded with AgNPs are reported. The Petri-side surface showed a more compact structure as compared to the air-side surface due to the contact with the polystyrene substrate that probably induced a compression of the pores (data not shown). All porous scaffolds showed a typical foam-like morphology with highly interconnected pores on the sections. Mean pore diameters of the fractured sections were 27.7±2.4 μm, 30±2.5 μm, 16±2.03 μm and 13±2.9 μm for CS/GPTMS_DSP, CS/GPTMS_DSP_AgNP5, CS/GPTMS_DSP_AgNP10 and CS/GPTMS_DSP_AgNP15 membranes. The pores showed a spherical shape and a decreasing size and density on the surface with increasing the initial AgNPs amount from 5 to 15 wt.%.

SEM images of fracture sections and surfaces of CS/GPTMS_DSP and GS loaded samples are reported in figure 2. Spherical, interconnected pores were observed both on the surface and on the section of CS/GPTMS_DSP_GS having a pore size dimension of 26.7±1.2 μm. Microstructure remodelling of CS/GPTMS_DSP_GS surface occurred after the rehydration and re-lyophilization processes used for the GS loading treatment: new pores with higher size and formation of sheets on the surface (reducing the interconnectivity) compared to control samples were detected and were associated to the removal of ice crystals during the second freeze-drying step. SEM analysis also evidenced the deposition and homogeneous distribution of the antibiotic agent into the bulk of the scaffold (insert in figure 2D).

Membrane pore size was investigated since pore distribution is known to affect cell and nutrient permeability. It has been reported that highly open porous polymer matrices are required for high-density cell infiltration, as well as sufficient nutrient and oxygen supply to the cells in the scaffold [37]. Pore sizes of 5-10 μm are favorable for vascularization while a multi-pore size membrane (212–250 μm, 250–300 μm, 355–500 μm) has been investigated to guarantee a better environment for cell proliferation, compared with the uniform-pore size scaffold [37]. On the basis of these considerations, CS/GPTMS_DSP_AgNP5, CS/GPTMS_DSP_AgNP10 and CS/GPTMS_DSP_GS could be ideal candidate materials for the production of porous membranes for wound healing in chelonians. However, a selection of the optimal dressing also required an evaluation of the mechanical performance and of the water uptake behaviour of porous samples.

EDS analysis was performed on CS/GPTMS_DSP, CS/GPTMS_AgNP5, CS/GPTMS_AgNP10 and CS/GPTMS_AgNP15 porous membranes to evaluate the distribution of AgNPs on the surfaces and sections of samples. Figure 3 reports the EDS element-mapping on the sections and surfaces for control and AgNPs loaded CS/GPTMS_DSP samples, respectively. EDS spectra of AgNPs loaded samples showed the characteristic elements of CS (C and O) and peaks corresponding to Si, Na and P elements associated both to the presence of GPTMS and DSP

crosslinkers (data not shown). The green spots corresponding to Ag element were uniformly dispersed both on the sections (figure 3B, C, D) and surfaces (figure 3F, G, H) of CS/GPTMS_DSP_AgNPs5, CS/GPTMS_DSP_AgNPs10 and CS/GPTMS_DSP_AgNPs15 samples.

3.2 Thermogravimetric analysis (TGA)

To further explore the interaction between CS/GPTMS_DSP and the two antibacterial agents (AgNPs and GS), the prepared membranes were characterized by TGA from 40°C to 800 C. The typical DGA curves of AgNPs and GS loaded membranes are reported in figures 4 and 5, respectively. Both the thermal curves clearly exhibited two distinctive thermal decomposition patterns (figure 4 and figure 5): the first decomposition step started from about 90°C and continued to above 150 °C and the second weight loss was observed in the temperature range between 180-550 °C. The initial thermal decomposition is mainly due to the evaporation of the water retained in the membranes and the second thermal event is attributed to the decomposition (oxidative and thermal) of the CS membrane matrix, which was completely destroyed around at temperature 550 °C. In addition, specimens exhibited small shoulders at 375 °C to 550 °C associated with the thermal destruction of GPTMS and DSP used as crosslinkers.

As shown in figure 4, after the addition of AgNPs, the onset temperature for the water evaporation and thermal decomposition of CS/GPTMS_DSP_AgNP5, CS/GPTMS_DSP_AgNP10 and CS/GPTMS_DSP_AgNP15 membranes delayed slightly to higher temperatures, indicating the increase in water holding capacity and thermal stability, which is mainly due to the presence of heat stable metallic Ag [38] (figure 4). The residual percentages of weight for CS/GPTMS_DSP, CS/GPTMS_AgNP5, CS/GPTMS_AgNP10 and CS/GPTMS_AgNP15 were 48.3%, 58.4%, 56.5% and 57.2%, respectively, and they are mainly due to the formation of inorganic compounds after decomposition containing C, N and O and to the presence of Ag nanoparticles into membranes. Table 1 reports the maximum water evaporation temperature (T_{we}), the maximum degradation rate temperature (T_d) of CS based samples and the corresponding weight losses. No differences were observed by increasing AgNPs amount from 5 to 15 wt. %. TGA analysis confirmed the improvement of the thermal stability of CS porous membranes after the addition of AgNPs.

Figure 5 reports the DGA curve of control and CS/GPTMS_DSP_GS samples. The incorporation of GS into CS/GPTMS_DSP membranes did not affect the thermal behavior of samples. CS/GPTMS_DSP_GS showed a first thermal degradation at around 140 °C and a second stage, associated to the thermal and oxidative decomposition of CS and to the vaporization and elimination of volatile products, starting at 210 °C and reaching a maximum at 630 °C with a total weight loss of 43.7%. CS decomposition masked GS thermal degradation which is known to partially take place in the 200–500 C interval and to have a final oxidation between 500 °C and 650° C [39].

3.3 Mechanical properties

Tensile and compressive tests were performed on wet state samples to mimic physiological environment and clinical procedures as, for the in vivo implantations on chelonians, membranes are soaked with 0.9 % NaCl solutions prior to implantation to have an increase in membranes flexibility resulting in an easy manipulation.

3.3.1 Tensile test

Tensile tests were performed on CS/GPTMS_DSP, CS/GPTMS_AgNP5, CS/GPTMS_AgNP10, CS/GPTMS_AgNP15 and CS/GPTMS_DSP_GS porous membranes in wet conditions to determine the effect of the antibacterial agents on sample stiffness. All CS based membranes showed an elasto-plastic behaviour at low strains (lower than 10%) where stress values increased linearly with strain increase. For strains >10%, the stress increased slowly until failure occurred (data not shown).

Addition of AgNPs resulted in a stiffening of the membranes (table 2) confirming the reinforcing effect of the nanoparticles in the polymeric matrix, which is consistent with literature data [38, 40]. In details, the elastic modulus of samples containing Ag nanoparticles differed significantly from the control (*$p<0.05$ for CS/GPTMS_DSP_AgNP5 and CS/GPTMS_DSP_AgNP10; **$p<0.01$ for CS/GPTMS_DSP_AgNP15). With increasing content of AgNPs, the E increased to a value ranging from 0.400-0.460 MPa (for CS/GPTMS_DSP_AgNP5 and CS/GPTMS_DSP_AgNP10) to 1.834±0.693 MPa (CS/GPTMS_DSP_AgNP15). Moreover, CS/GPTMS_DSP_AgNP15 elastic modulus value was significantly different from CS/GPTMS_DSP_AgNP5 and CS/GPTMS_DSP_AgNP10 ones (*$p<0.05$ and **$p<0.01$ respectively). The increase stiffness of CS/GPTMS_DSP_AgNP15 could be ascribed to the decrease of the degree of sample porosity caused by the higher amount of Ag nanoparticles. A significant increase (*$p<0.05$) of E value was also observed for CS/GPTMS_DSP_GS samples (1.180±0.560 MPa) compared to CS/GPTMS_DSP. This result is probably associated to the morphological changes caused by freeze-drying process after GS incorporation, as discussed in paragraph 3.1.

All the investigated samples showed an high flexibility and an easy manipulation after immersion in physiological fluids. Furthermore, measured E values are in the range of 0.3-2.5 MPa comparable with the skin range value reported in the literature [41, 42] showing a biomimetic mechanical behaviour.

3.3.2 Compressive test

Figure 6 shows the compressive stress–strain curves for the AgNPs loaded CS/GPTMS_DPS porous scaffolds. CS/GPTMS_DSP containing Ag nanoparticles were characterized by a linear elastic regime at low deformations (elongation 0-10%) and a collapse regime at higher deformations (between 10- 20%). Samples did not reach final fracture and underwent densification. Data for wet CS/GPTMS_DSP specimens were not reported since load values were too low to be acquired by the equipment used. The addition of different amount of AgNPs showed an increase of the E and E* (table 3) by obtaining values around 0.030 MPa and 0.035 MPa for CS/GPTMS_DSP_AgNP5 and CS/GPTMS_DSP_AgNP10 to 0.070±0.012 MPa and 0.093±0.007 for CS/GPTMS_DSP_AgNP15.

In addition, the stress and strain values of transition from linear to collapse regime (σ^* and ε^*) were observed for higher stress values (0.009±0.001 MPa for CS/GPTMS_DSP_AgNP5 to about 0.011 MPa for CS/GPTMS_DSP_AgNP10 and CS/GPTMS_DSP_AgNP15) and for increased elongations (from about 20 % for CS/GPTMS_DSP_AgNP5 and CS/GPTMS_DSP_AgNP10 to 12.848±2.640 for CS/GPTMS_AgNP15). The increase of E and E* values for CS/GPTMS_DSP_AgNP15 samples (statistical significant compared to CS/GPTMS_DSP_AgNP5 samples, $*p<0.05$) was due to the mechanical reinforcement associated with the addition of Ag nanoparticles and the decrease of sample porosity.

The characteristic stress-strain curve of soft and porous materials was also observed for CS/GPTMS_DSP_GS samples (data not shown). After the introduction of GS to CS/GPTMS_DSP, E, E*, σ^* and ε^* were comparable to CS/GPTMS_DSP_AgNP15 obtaining values of 0.088±0.038 MPa, 0.093±0.029 MPa, 0.010±0.000 MPa and 12.848±3.125 %, respectively (table 3). The structure modification following the incorporation of GS into the CS based porous membranes seem to affect the mechanical properties of samples.

3.4 Water uptake and dissolution tests

Water uptake and dissolution degree of CS/GPTMS_DSP samples loading Ag nanoparticles and GS are shown in figure 7 and figure 8, respectively.

Figure 7A reports the water uptake of CS/GPTMS_DSP, CS/GPTMS_DSP_AgNP5, CS/GPTMS_DSP_AgNP10 and CS/GPTMS_DSP_AgNP15. A comparison of the swelling percentage of AgNPs loaded samples to CS/GPTMS_DSP revealed that the water uptake was similar for all samples at each time point. In details, porous membranes increased considerably their weight immediately after 1 hour of immersion in PBS solution reaching values of water uptake of 1219±19 %, 1356±9 %, 1174±126 % and 1150±193 %, for CS/GPTMS_DSP, CS/GPTMS_DSP_AgNP5, CS/GPTMS_DSP_AgNP10 and CS/GPTMS_DSP_AgNP15 respectively. Then, the swelling values remained stable till the end of the experiment.

The dissolution profiles of AgNPs loaded CS based samples after 56 days of immersion in PBS are presented in figure 7B. CS/GPTMS_DSP, CS/GPTMS_DSP_AgNP5, CS/GPTMS_DSP_AgNP10 and CS/GPTMS_DSP_AgNP15 membranes decreased their weight of 11.0±2.0 %, 9.9±3.5 %, 9.0±0.7% and 11.6±2.0 % after 1 day incubation in PBS, respectively. The initial high weight loss was associated to the release of DSP salts into PBS solution. The weight loss values remained stable until14 days, then a moderate increase was measured after 28-56 days. Final dissolution values of 25.2±3.3 % for CS/GPTMS_DSP, 21.8±1.3 % for CS/GPTMS_DSP_AgNP5, 21.7±0.2 % CS/GPTMS_DSP_AgNP10 and 22.5±0.8 % for CS/GPTMS_DSP_AgNP15 were reached after 56 days incubation in PBS. No significant differences were observed between all samples at each time point.

In figure 8A, the water uptake of porous membranes was measured to examine the changes of properties of CS/GPTMS_DSP in presence of GS. The water uptake of samples without GS was higher compared to CS/GPTMS_DSP_GS. The swelling degree of GS loaded CS/GPTMS_DPS reached values of 863±205 % after 1 hour incubation in PBS and a slightly increase was observed till 24 hours of immersion in physiological solution (973±165 %). Significant differences were observed between control and CS/GPTMS_DSP_GS at the first two time points of experiment (*$p < 0.05$). The lower water absorption behavior of CS/GPTMS_DSP_GS is related to the microstructure remodeling of the surface that occurs after antibiotic agent loading.

Figure 8B shows the percentage weight loss of CS/GPTMS_DSP and CS/GPTMS_DSP_GS membranes. A comparable weight reduction was measured for CS/GPTMS_DSP and CS/GPTMS_DSP_GS until 7 days. Then, at days 14, a significant differences compared to CS/GPTMS_DSP (***$p<0.001$) was measured and it can be attributed to the GS release from the polymer matrix that increased the weight loss of GS loaded membranes. On the contrary, after 56 days, samples containing GS showed a weight loss of about 20% while an higher degradation was measured for CS/GPTMS_DSP (*$p<0.05$).

3.5 Drug release evaluation

The GS release from CS/GPTMS_DSP porous membranes was evaluated in vitro quantifying the amount of GS in the collected medium. Figure 9 shows the cumulative release after 1, 3, 6 and 24 hours and at 2, 5, 7, 14, 28 and 56 days. An initial burst release was observed at 24 hours (about 70% with respect to the GS loaded into the membranes) followed by a moderate release over the subsequent days (around 0.55% each day). During the first 24 hours the release is mainly driven by diffusive mechanism and then, the CS/GPTMS_DSP_GS degradation allowed the release of a constant and moderate amount of GS.

The local delivery of antibiotics at injured site is a preferred option to systemic administration since (i) it reduces the risk of systemic toxicity such as cell and organ toxicity [43, 44], (ii) it provides tissue compatibility and low occurrence

of bacterial resistance [45] and (iii) it overcomes the problem of ineffective systemic antibiotic therapy resulting from poor blood circulation. The release kinetics measured for CS/GPTMS_DSP_GS membranes having a high initial GS release will enhance the antimicrobial effect, reducing the bacterial population on the wound site from the first day after implantation.

3.6 Antibacterial tests

In order to quantify the effect of GS and AgNPs on both Gram-negative (*Escherichia coli, Pseudomonas aeruginosa* and *Proteus mirabilis*) and Gram-positive (*Staphylococcus aureus Enterococcus faecalis)* bacteria, time-killing assay was performed on CS/GPTMS_DSP, CS/GPTMS_DSP_GS and CS/GPTMS_DSP_AgNP10 by measuring the reduction of the number of CFU recovered at 18 hours. CS/GPTMS_DSP_AgNP10 samples were selected as optimized scaffolds since the AgNPs amount of 10 wt.%. was the highest loaded quantity that did not affect the sample porosity on the surface. Figure 10 shows the qualitative antibacterial efficacy exerted by the three membranes on *Staphylococcus aureus.* The results of the antibacterial screening of the tested scaffolds are presented in figure 11. The AgNPs impregnated CS membranes showed a bactericidal effect on all bacteria: growth of *Staphylococcus aureus, Escherichia coli, Enterococcus faecalis, Pseudomonas aeruginosa* and *Proteus mirabilis* was reduced by logarithmic orders of 3.4, 1.5, 1.8, 2.3 and 1.6, respectively compared to CS/GPTMS_DSP. GS loaded CS/GPTMS_DSP membranes revealed total bactericidal activity against *Escherichia coli, Staphylococcus aureus* and *Enterococcus faecalis* but they were unable to inhibit bacterial propagation in case of *Pseudomonas aeruginosa* strain as compared to CS/GPTMS_DSP. *Proteus mirabilis* was reduced by logarithmic orders 1.27 respect to CS/GPTMS_DSP, showing results comparable to that obtained by CS/GPTMS_DSP_AgNP10. The most effective membrane against *Escherichia coli, Staphylococcus aureus* and *Enterococcus faecalis* strains was the one impregnated with GS, while the highest antibacterial activity against *Pseudomonas aeruginosa* was found for membranes containing AgNPs. The simultaneous loading of two agents (GS and AgNPs) on CS membranes will guarantee to improve the antibacterial effect against a broad spectrum of strains reducing the risk of infections that can consequently compromise the healing process.

3. Conclusion

Biodegradable wound dressings based on CS porous membranes with improved antimicrobial activities were developed to treat infected injures in animals. Chelonian shell injuries were selected as initial models to test the efficacy of this innovative treatment. Porous CS membranes containing GS or different ratios of AgNPs (5, 10 and 15% wt./wt.) were obtained by freeze-drying technique. Mechanical characterization was performed on samples showing that the incorporation of AgNPs or GS enhanced the stiffness of CS/GPTMS_DSP samples. Moreover, a strict correlation was

observed between the Young modulus and the amount of AgNPs incorporated into the membranes: E increased as the AgNPs concentration incresed from 5% wt. to 15 wt.%. The high swelling degree, which is one of the important factor for reducing the risk of wound dehydration, was observed for all antimicrobial agent loaded samples reaching final values of about 1200-1300% and 950% for AgNPs and GS loaded membranes after 24 hours of incubation in physiological solution, respectively. However, the incorporation of the antimicrobial agents into CS/GPTMS_DSP affected the surface morphologies of porous membranes. Pore occlusion on the surface of CS based membranes containing AgNPs was detected increasing the amount of AgNPs. For this reason, CS/GPTMS_DSP_AgNP10 was selected as ideal candidate for this application field since it joins the good bacteriocide activities of Ag without affecting the CS based membranes structures as observed for 15% amount of Ag. After GS loading, new pores with higher size and formation of sheets on the surface (reducing the interconnectivity) were formed following rehydration and re-lyophilization processes used for the GS loading treatment. GS release profile from CS/GPTMS_DSP_GS demonstrated high burst release of the antibiotics in the first 24 hours (about 70% with respect to the GS loaded into the membranes), followed by gradual release at a decreasing rate over time.

Finally, GS and AgNPs (10% wt./wt.) effect on bacterial inhibition was investigated showing that the presence of either AgNPs or GS improved the antimicrobial activity of CS based porous membranes. GS loaded samples were highly efficient against *Escherichia coli*, *Staphylococcus aureus* and *Enterococcus faecalis* strains while CS/GPTMS_DSP_AgNP10 increased the inhibitory effect against *Pseudomonas aeruginosa* and *Proteus mirabilis* bacteria compared to control and GS loaded samples. Preliminary *in vivo* results showed effectiveness of the membranes [48]: CS/GPTMS_DSP_GS membranes were implanted for 21 days on 12 Hermann's tortoises (*Testudo hermanni*) with various shell injuries. Mould developed in two cases, and membranes were removed and re-implanted. All the animals recovered uneventfully [48]. Future works will be addressed to *in vivo* test of composite membranes based on CS impregnated with both AgNPs and antibiotics GS with the aim to improve the antibacterial activity against a broad spectrum of strains.

Acknowledgment

Clara Mattu is acknowledge for SEM analysis.

Figures

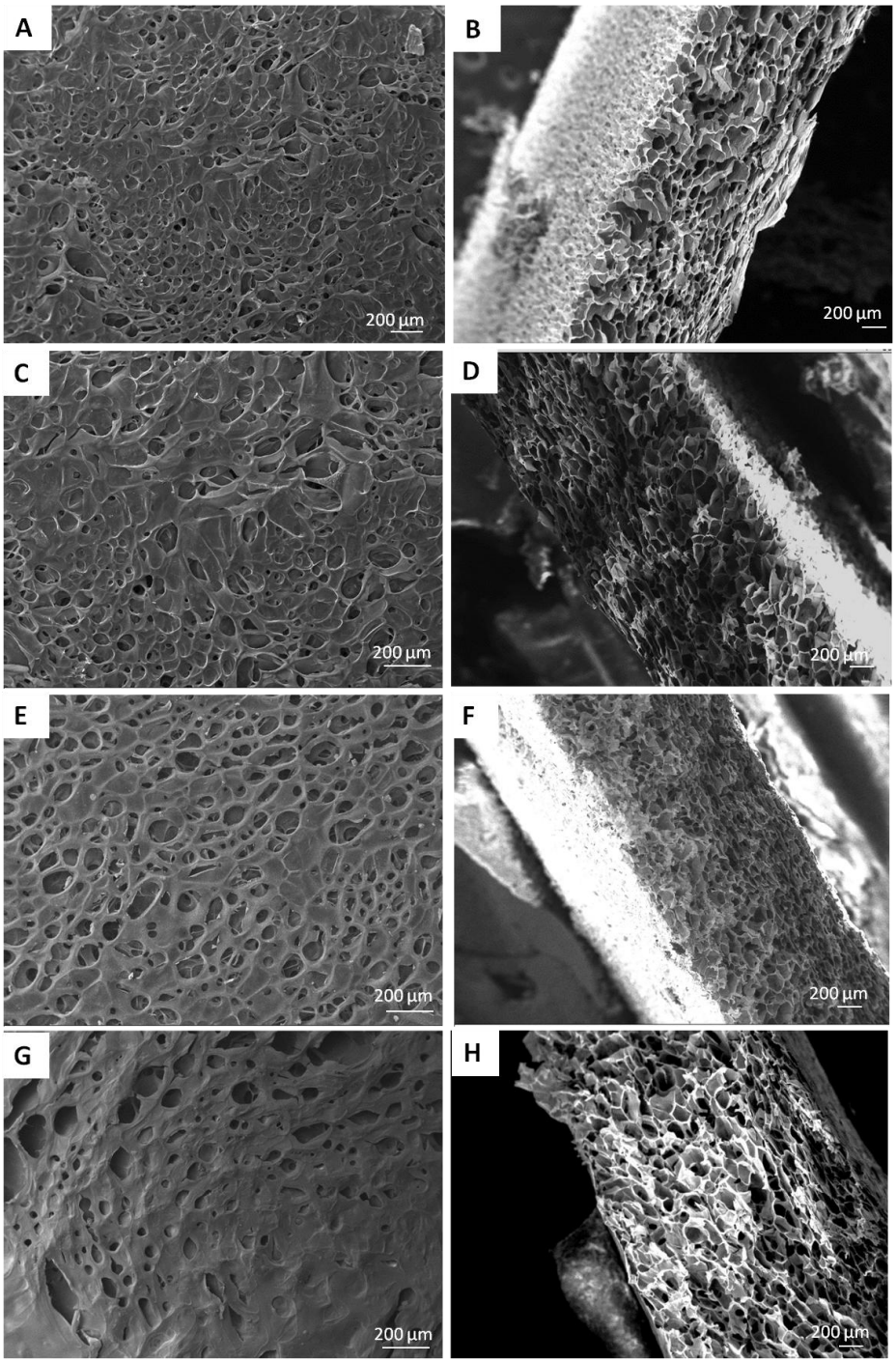

Figure 1. SEM micrographs of CS based membrane surfaces (A, C, E, G) and sections (B, D, F, H) after AgNPs addition: (A, B) CS/GPTMS_DSP; (C, D) CS/GPTMS_DSP_AgNP5; (E,F) CS/GPTMS_DSP_AgNP10; (G, H) CS/GPTMS_DSP_AgNP15.

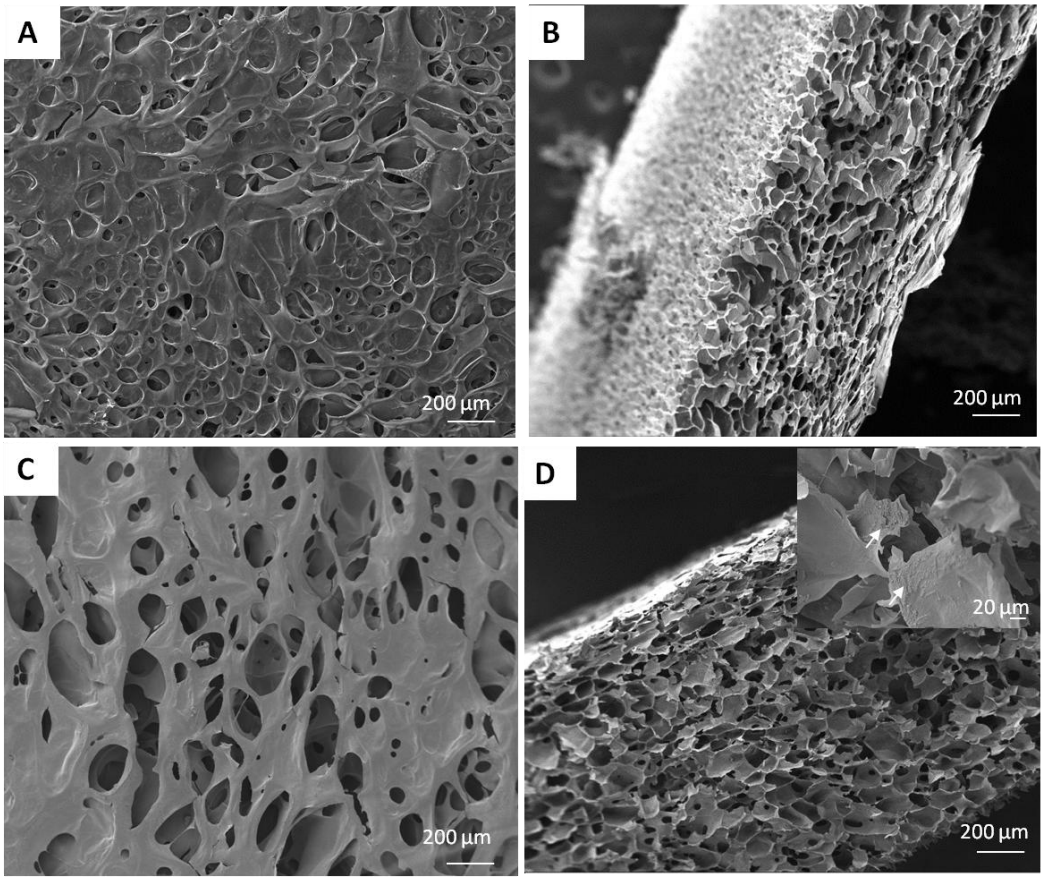

Figure 2. SEM micrographs of CS/GPTMS_DSP (A,B) and CS/GPTMS_DSP_GS (C, D) membrane surfaces (A, C) and sections (B, D). Arrows indicated the presence of GS.

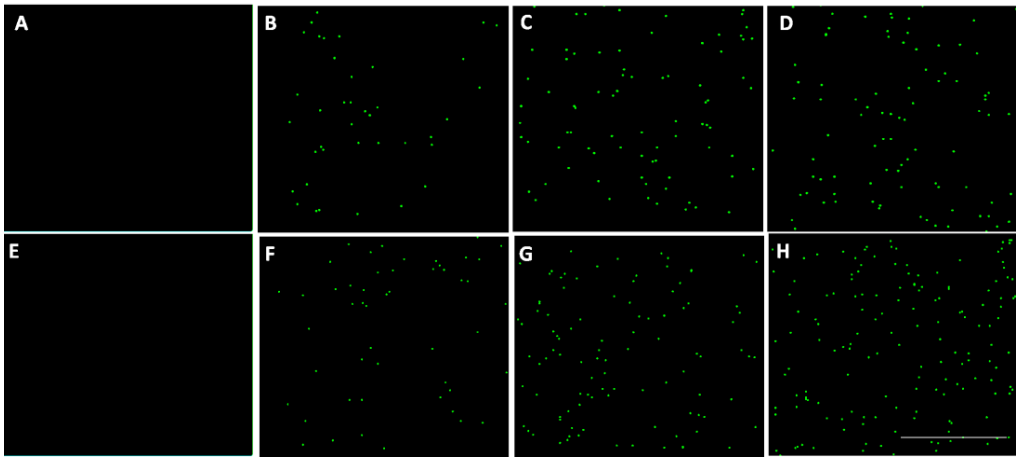

Figure 3. EDS spectra of sections (A, B, C, D) and surfaces (E, F, G, H) of CS based porous membrane: (A, E) CS/GPTMS_DSP; (B, F) CS/GPTMS_DSP_AgNP5; (C, G) CS/GPTMS_DSP_AgNP10; (D, H) CS/GPTMS_DSP_AgNP15. Scale bar: 200 µm. Green spots represented Ag element.

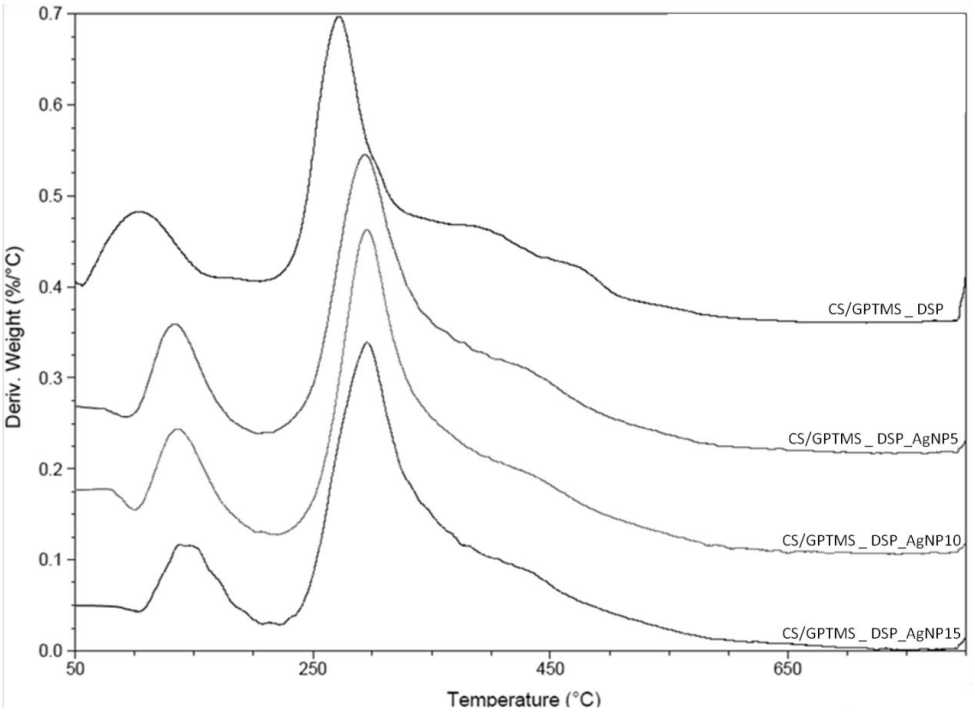

Figure 4. First derivative of TGA curves of CS/GPTMS_DSP, CS/GPTMS_DSP_AgNP5, CS/GPTMS_DSP_AgNP10 and CS/GPTMS_DSP_AgNP15 porous membranes.

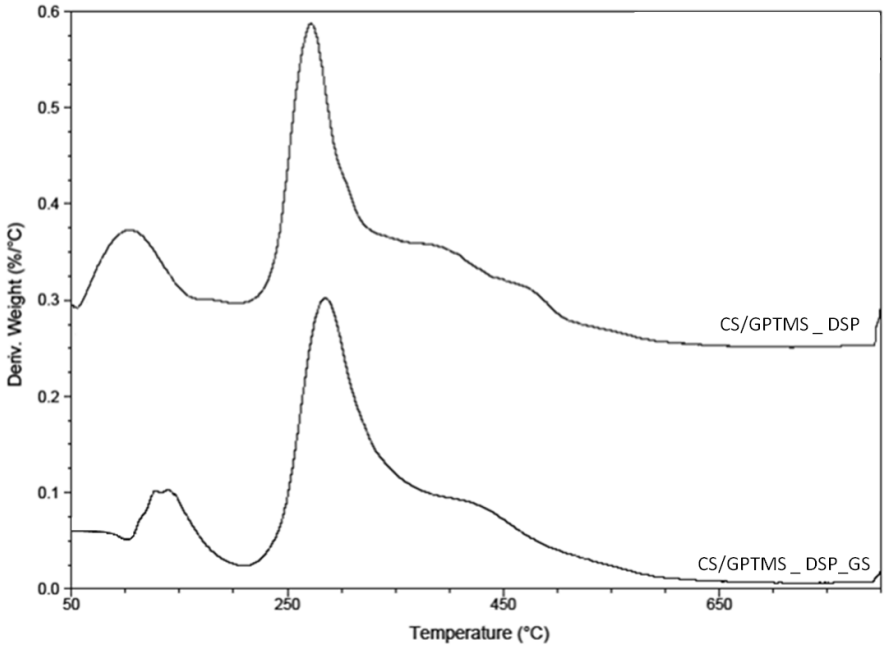

Figure 5. First derivative of TGA curves of CS/GPTMS_DSP and CS/GPTMS_DSP_GS porous membranes.

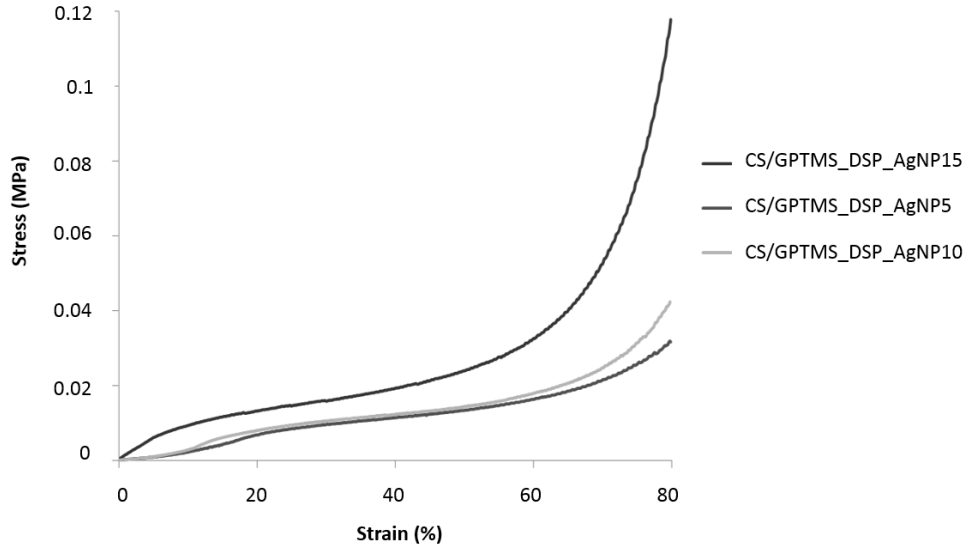

Figure 6. Compression stress versus strain curves of CS/GPTMS_DSP_AgNP5, CS/GPTMS_DSP_AgNP10 and CS/GPTMS_DSP_AgNP15. Data for wet CS/GPTMS_DSP specimens were not reported since load value reached were too low to be acquired by the equipment used.

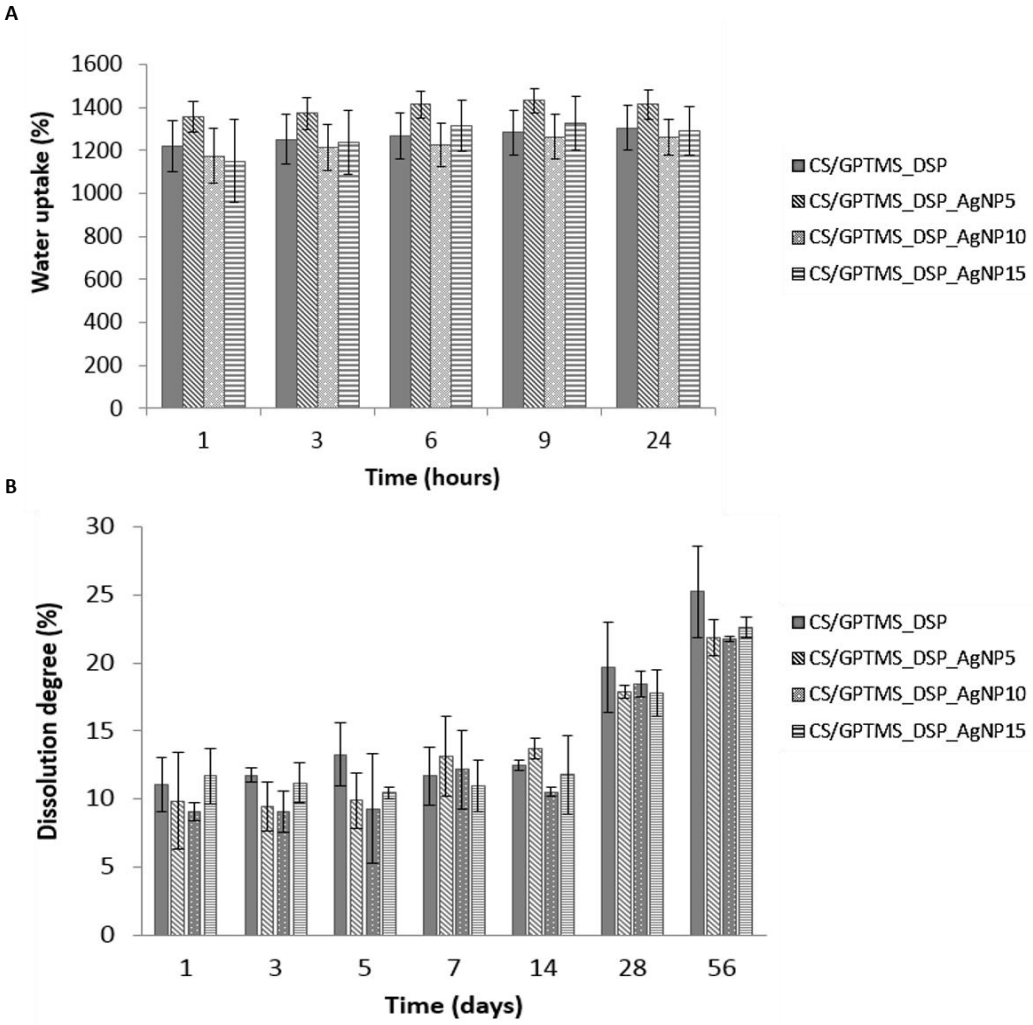

Figure 7. Water uptake (A) and dissolution degree (B) of CS/GPTMS_DSP, CS/GPTMS_DSP_AgNP5, CS/GPTMS_DSP_AgNP10 and CS/GPTMS_DSP_AgNP15 porous membranes in PBS as a function of time**.** Column heights correspond to the mean values. Bars indicate standard deviations (n = 3).

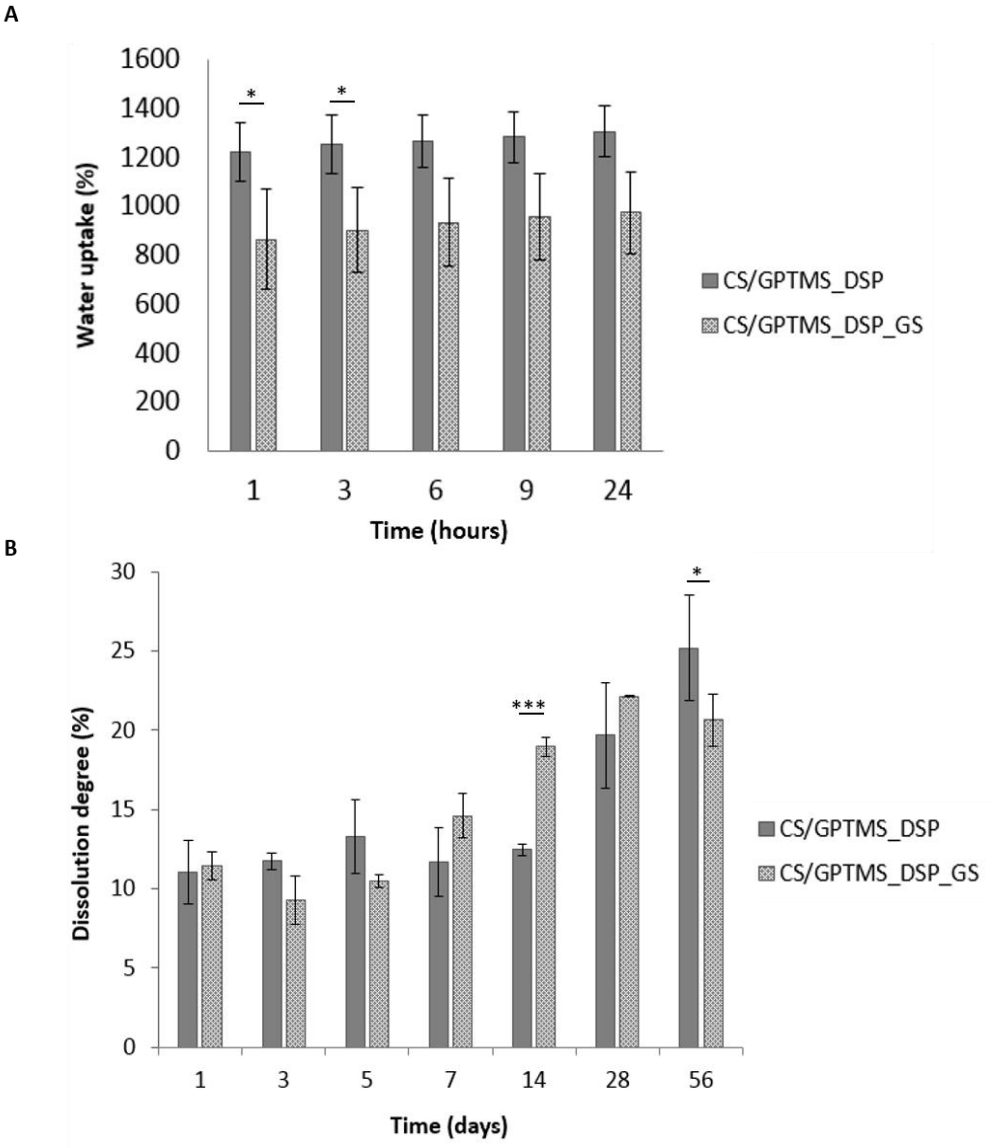

Figure 8. Water uptake (A) and dissolution degree (B) of CS/GPTMS_DSP and CS/GPTMS_DSP_GS porous membranes in PBS as a function of time**.** Column heights correspond to the mean values. Bars indicate standard deviations (n = 3).*p< 0.05, ***p<0.001.

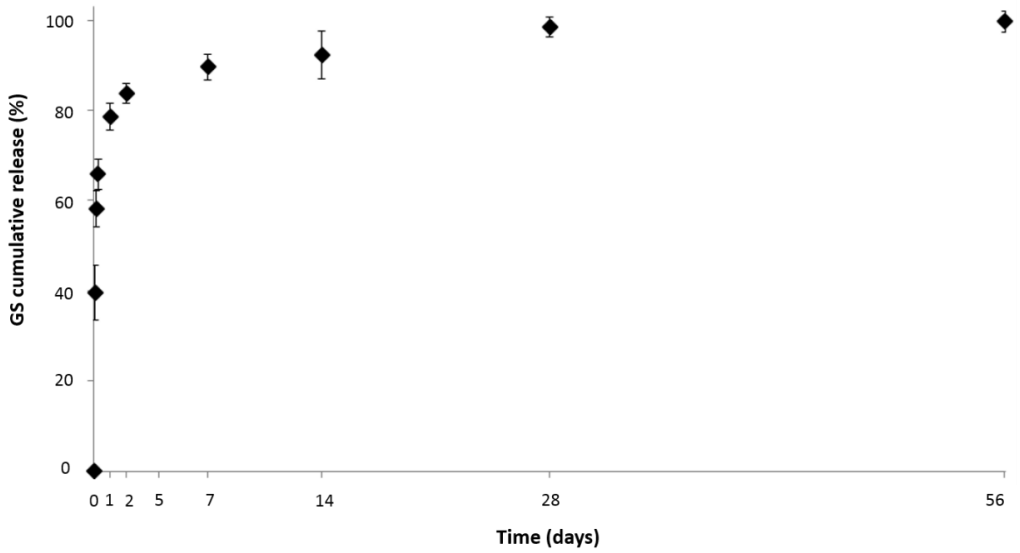

Figure 9. GS release after 1, 3, 6, 24 hours and 2, 5, 7, 14 , 28 and 56 days. The curve reports the percentage cumulative release values normalized respect to the initial amount of the GS incorporated within the CS/GPTMS_DSP_GS porous membranes. Markers correspond to the mean values. Bars indicate standard deviations (n = 3).

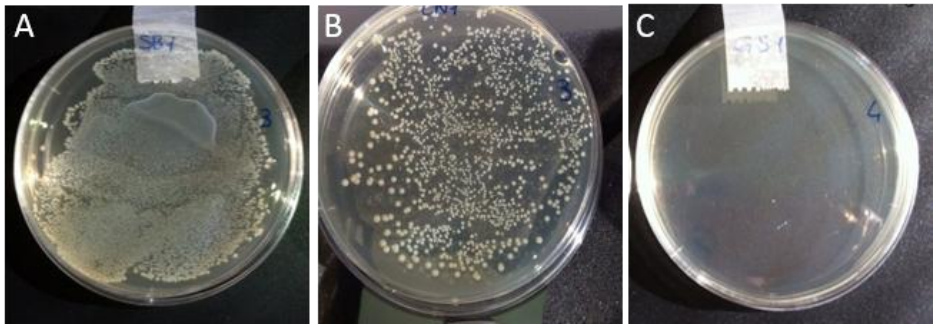

Figure 10. *S. aureus* growth in contact with control (A), CS/GPTMS_DSP_GS (B) and CS/GPTMS_DSP_AgNP10 (C) membranes without MHB dilutions.

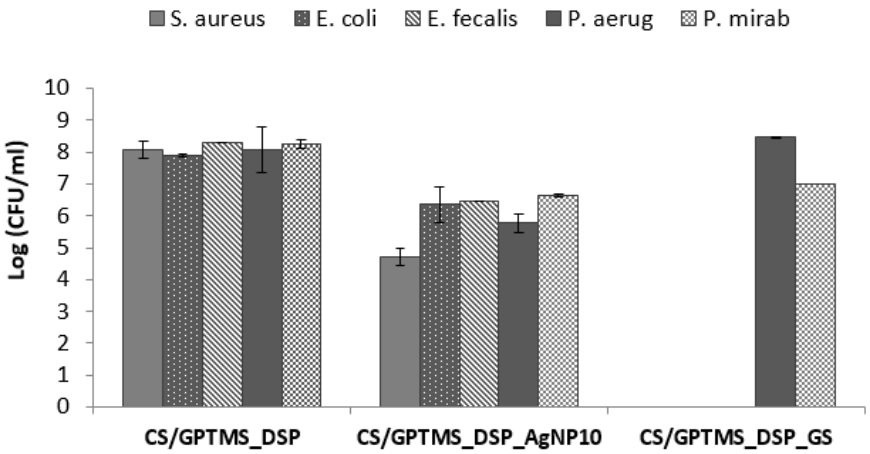

Figure 11. Kinetics of growth inhibition of *S. Aureus, E. Coli, E. Fecalis, P. aeruginosa* and *P. mirabilis* in presence CS/GPTMS_DSP, CS/GPTMS_DSP_GS and CS/GPTMS_DSP_AgNP10.

Tables

Table 1. Maximum water evaporation temperature (T_{we}), maximum degradation rate temperature (T_d) and corresponding and total weight loss for CS based samples.

Sample	T_{we} (°C)	T_{we} Weight loss (%)	T_d (°C)	T_d Weight loss (%)	Total weight loss (%)
CS/GPTMS_DSP	87.0	10.2	273	41.5	51.7
CS/GPTMS_DSP_AgNP5	137.8	6.0	291.8	35.6	41.6
CS/GPTMS_DSP_AgNP10	138.6	6.5	291.8	36.9	43.5
CS/GPTMS_DSP_AgNP15	138.9	5.8	292.0	37.0	42.8

Table 2. Elastic modulus calculated from the corresponding stress-strain curves of wet CS/GPTMS_DSP based samples (average value ± standard deviation).

Sample	E_{wet} (MPa)
CS/GPTMS_DSP	0.085±0.010
CS/GPTMS_DSP_AgNP5	0.405±0.185
CS/GPTMS_DSP_AgNP10	0.397±4.14
CS/GPTMS_DSP_AgNP15	1.834±0.693
CS/GPTMS_DSP_GS	1.180±0.560

Table 3 The elastic modulus (E), the collapse modulus (E*) and the collapse stress and strain (σ* and ε*, respectively) of CS/GPTMS membranes.

Sample	E (MPa)	E* (MPa)	σ* (MPa)	ε*(%)
CS/GPTMS_DSP_AgNP5	0.032±0.007	0.034±0.005	0.009±0.001	23.720±3.548
CS/GPTMS_DSP_AgNP10	0.030±0.023	0.040±0.021	0.011±0.001	19.300±9.957
CS/GPTMS_DSP_AgNP15	0.070±0.012	0.093±0.007	0.011±0.000	12.848±2.640
CS/GPTMS_DSP_GS	0.088±0.038	0.093±0.029	0.010±0.000	12.848±3.125

References

1. Fleming, G., *Clinical technique: chelonian shell repair.* Journal of Exotic Pet Medicine, 2008. **17**(4): p. 246-258.
2. Alibardi, L., *Ultrastructural and immunohistochemical observations on the process of horny growth in chelonian shells.* Acta Histochem, 2006. **108**(2): p. 149-62.
3. Jackson, O.F., *Tortoise shell repair over two years.* Vet Rec, 1978. **102**(13): p. 284-5.

4. Frye, F.L., *Clinical evaluation of a rapid polymerizing epoxy resin for repair of shell defects in tortoises.* Vet Med Small Anim Clin, 1973. **68**(1): p. 51-3.
5. Zeman, W.V., F.G. Falco, and J.J. Falco, *Repair of the carapace of a box turtle using a polyester resin.* Lab Anim Care, 1967. **17**(4): p. 424-5.
6. Holt, P.E., *Healing of a surgically induced shell wound in a tortoise.* Vet Rec, 1981. **108**(5): p. 102.
7. Mader, D., Bennet, RA., Funk RS., *Reptile Medicine and Surgery* ed. M. DR2006, St Louis: Saunders/Elsevier. 581-630.
8. Mayer, J. and T. Donnelly, *Clinical Veterinary Advisor, Birds and Exotic Pets*, ed. M.J.a.D. TM2013: Elsevier Health Sciences.
9. Lafortune, M., et al., *Vacuum-assisted closure (Turtle VAC) in the management of traumatic shell defects in chelonians.* Journal of Herpetological Medicine and Surgery, 2005. **15**: p. 4-8.
10. Mitchell, M.A. and T.N. Tully, *Manual of Exotic Pet Practice.*2009: Elsevier Health Sciences.
11. Amable, P.R., et al., *Platelet-rich plasma preparation for regenerative medicine: optimization and quantification of cytokines and growth factors.* Stem Cell Res Ther, 2013. **4**(3): p. 67.
12. Pelizzone, I., et al. *Shell fracture repair a comparison of different methods and the use of PRP (Platelet-rich-plasma)*. in *Internationl Conference on Reptile and amphibian Medicine*. 2012. Cremona, Italy.
13. Mathews, K.A. and A.G. Binning, *Wound management using honey.* Compend. Con. Edu, 2002. **24**(1): p. 53-59.
14. Norton, T., et al. *Medical and surgical management of automobile and boat strike trauma in Diamondback Terrapins and marine turtles*. 2010.
15. Mitchell, M.A. and O. Diaz-Figueroa, *Wound management in reptiles.* Vet Clin North Am Exot Anim Pract, 2004. **7**(1): p. 123-40.
16. Richards, J., *Metal bridges-a new technique of turtle shell repair.* J Herp Med Surg, 2001. **11**(4): p. 31-34.
17. Fowler, A. and N. Magelakis, *Shell fracture repair using glass ionomer cement in the long-neck tortoise (Chelodina longicollis)*, in *Wildlife Disease Association-Australian section*2003: Healesville, Victoria.
18. Kishimori, C. and G. Lewbart, *Chelonian shell fracture repair techniques.* Exotic DVM, 2001. **3**(5): p. 35-41.
19. Vella, D., *Reports on effective modern shell repair techniques for turtles*, in *The Veterinarian* S.M.P.P. Ltd, Editor 2006: Sidney.
20. Tobias, K. *Wound management*. in *SCIVAC*. 2014. Rimini, Italy.
21. Argenta, L.C. and M.J. Morykwas, *Vacuum-assisted closure: a new method for wound control and treatment: clinical experience.* Ann Plast Surg, 1997. **38**(6): p. 563-76; discussion 577.
22. Gabriel, A., et al., *A clinical review of infected wound treatment with Vacuum Assisted Closure (V.A.C.) therapy: experience and case series.* Int Wound J, 2009. **6 Suppl 2**: p. 1-25.
23. Eppley, B.L., J.E. Woodell, and J. Higgins, *Platelet quantification and growth factor analysis from platelet-rich plasma: implications for wound healing.* Plastic and Reconstructive Surgery, 2004. **114**(6): p. 1502-8.
24. Coke, R.L. and P.A. Reyes-Fore. *Treatment of a Radiated tortoise (Geochelone Radiata) with Komodo dragon (Varanus Komodoensis) bite wouds*. 2004.
25. Me, N., et al., *Antibacterial activity of chitosan coated Ag-loaded nano-SiO2 composites* Carbohydrate Polymers, 2009. **78**(1): p. 54-59.
26. Sanpui, P., et al., *The antibacterial properties of a novel chitosan-Ag-nanoparticle composite.* International Journal of Food Microbiology, 2008. **124**(2): p. 142-6.
27. Kim, S., et al., *Oxidative stress-dependent toxicity of silver nanoparticles in human hepatoma cells.* Toxicology in Vitro, 2009. **23**(6): p. 1076-84.
28. Kwakman, P.H., et al., *Medical-grade honey enriched with antimicrobial peptides has enhanced activity against antibiotic-resistant pathogens.* Eur J Clin Microbiol Infect Dis, 2011. **30**(2): p. 251-7.
29. Kwakman, P.H., et al., *How honey kills bacteria.* Faseb Journal, 2010. **24**(7): p. 2576-82.
30. Rudin, A., et al., *Antibacterial activity of gentamicin sulfate in tissue culture.* Appl Microbiol, 1970. **20**(6): p. 989-90.

31. Falco, F.G., H.M. Smith, and G.M. Arcieri, *Nephrotoxicity of aminoglycosides and gentamicin.* J Infect Dis, 1969. **119**(4): p. 406-9.
32. O'Shea, R. and R.L. Ball. *Use of bovine tendon collagen for wound repair in Varanus komodoensis*. 2010.
33. Abdelrahman, T. and H. Newton, *Wound dressings: principles and practice.* Surgery (Oxford), 2011. **29**(10): p. 491-495.
34. Boateng, J.S., et al., *Wound healing dressings and drug delivery systems: a review.* J Pharm Sci, 2008. **97**(8): p. 2892-923.
35. Takei, T., et al., *Synthesis of a chitosan derivative soluble at neutral pH and gellable by freeze-thawing, and its application in wound care.* Acta Biomaterialia, 2012. **8**(2): p. 686-693.
36. Muzzarelli, R.A.A., *Chitins and chitosans for the repair of wounded skin, nerve, cartilage and bone.* Carbohydrate Polymers, 2009. **76**(2): p. 167-182.
37. Lee, J.J., et al., *Investigation on biodegradable PLGA scaffold with various pore size structure for skin tissue engineering.* Current Applied Physics, 2007. **7**(1): p. 37-40.
38. Rhim, J.W., et al., *Preparation and characterization of bio-nanocomposite films of agar and silver nanoparticles: laser ablation method.* Carbohydr Polym, 2014. **103**: p. 456-65.
39. Vasile, B.S., et al., *Synthesis and characterization of a novel controlled release zinc oxide/gentamicin-chitosan composite with potential applications in wounds care.* International Journal of Pharmaceutics, 2014. **463**(2): p. 161-9.
40. Chang, P.R., et al., *Fabrication and characterisation of chitosan nanoparticles/plasticised-starch composites.* Food Chemistry, 2010. **120**(3): p. 736-740.
41. Agache, P.G., et al., *Mechanical properties and Young's modulus of human skin in vivo.* Arch Dermatol Res, 1980. **269**(3): p. 221-32.
42. Manschot, J.F. and A.J. Brakkee, *The measurement and modelling of the mechanical properties of human skin in vivo--II. The model.* Journal of biomechanics, 1986. **19**(7): p. 517-21.
43. Garric, X., M. Vert, and J.P. Moles, *[Development of new skin substitutes based on bioresorbable polymer for treatment of severe skin defects].* Ann Pharm Fr, 2008. **66**(5-6): p. 313-8.
44. Stashak T. S. , F.E., Othic A., *Update on Wound Dressings: Indications and Best Use*, C.T.E. Pract, Editor 2004. p. 148-163.
45. Kim, H.L., et al., *Evaluation of electrospun (1,3)-(1,6)-beta-D-glucans/biodegradable polymer as artificial skin for full-thickness wound healing.* Tissue Eng Part A, 2012. **18**(21-22): p. 2315-22.